#### **ORIGINAL ARTICLE**





# Development of a Method for Visualizing and Quantifying Thrombus Formation in Extracorporeal Membrane Oxygenators

Jenny S. H. Wang¹ 

· Amelia A. Rodolf¹ · Caleb H. Moon¹ · Ari Lauthner¹ · Helen H. Vu¹ · Sandra Rugonyi¹ · Anna J. Hansen² · Heather M. Mayes³ · Bishoy Zakhary⁴ · David Zonies⁵ · Ran Ran⁴ · Akram Khan⁴ · Denis Wirtz⁻,8,9,10,11 · Ashley L. Kiemen⁻,8,11,12,13 · Owen J. T. McCarty¹ · Joseph J. Shatzel¹,1⁴

Received: 20 September 2024 / Accepted: 30 March 2025 / Published online: 12 April 2025
This is a U.S. Government work and not under copyright protection in the US; foreign copyright protection may apply 2025

#### **Abstract**

**Purpose** Extracorporeal membrane oxygenation (ECMO) is a life-saving critical care technology that presents significant risks of medical device-associated thrombosis. We developed a complete method for collecting membrane oxygenators (membrane lung) from patients receiving ECMO treatment and quantitatively analyzing the distribution of thrombus formation within the membrane.

**Methods** We collected used membrane oxygenators from patients for processing and imaging with microcomputed tomography (microCT). We reconstructed the microCT data and performed image segmentation to identify regions of thrombus formation within these oxygenators. We performed density mapping to quantify thrombus volume across different regions of each oxygenator and within multiple oxygenator models.

**Results** Our method yields two-dimensional and three-dimensional visualization and quantification of thrombus deposition in ECMO. Analysis of the spatial distribution of platelet deposition, red blood cell entrapment, and fibrin formation within the fouled device provides insights into the structural patterns of oxygenator thrombosis.

**Conclusions** This method can enable quantification of oxygenator thrombosis which can be used for evaluating the effect of new biomaterial or pharmacological approaches for mitigating vascular device-associated thrombosis during ECMO.

 $\textbf{Keywords} \ \ \text{Thrombosis} \cdot \text{Medical device-associated thrombosis} \cdot \text{Extracorporeal membrane oxygenation} \cdot \text{Computed tomography}$ 

#### **Abbreviations**

CPB Cardiopulmonary bypass

ECMO Extracorporeal membrane oxygenation

H&E Hematoxylin and eosin
HU Hounsfield units

MicroCT Microcomputed tomography
PBS Phosphate-buffered saline
SEM Scanning electron microscopy

VA Veno-arterial VV Veno-venous

Associate Editor Edward Sander oversaw the review of this article.

Extended author information available on the last page of the article

#### Introduction

Extracorporeal membrane oxygenation (ECMO) provides critical care support during cardiac and respiratory failure [1]. Like a cardiopulmonary bypass (CPB) circuit, the ECMO circuit contains vascular access cannulas, a pump which performs the cardiac function, and an oxygenator which substitutes for respiratory function. Unlike CPB, which provides short-term support during cardiac surgery, ECMO provides long-term support for patients [2]. ECMO applications include management of severe respiratory failure or severe cardiogenic shock [3–5].

Despite providing organ support, ECMO imparts a significant risk of thrombosis, both within the device itself as well as within the patient, including pulmonary embolism and ischemic stroke [6]. Contact between blood and biomaterial surfaces that comprise the ECMO circuit can initiate and exacerbate thrombotic complications. For instance, select surfaces within the membrane oxygenator can initiate



and promote coagulation factor activation, protein adsorption, and platelet adhesion within the oxygenator, resulting in thrombogenesis. As many as 10-16% of ECMO patients experience membrane oxygenator thrombosis, and prolonged ECMO support may require frequent oxygenator replacements [3, 7]. Thrombosis within the oxygenator impedes blood flow and compromises gas exchange efficiency. In addition to thromboembolic complications, ECMO surfaces may contribute to disseminated intravascular coagulation, which consumes clotting factors and platelets, leading to hemorrhage [8, 9].

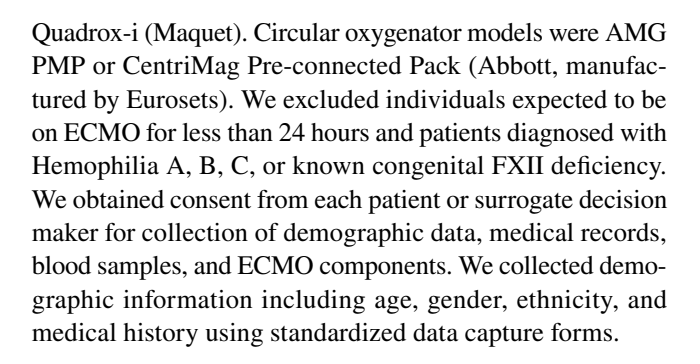
Thus, there is an urgent need for further research to understand thrombosis and bleeding during ECMO and to develop effective strategies to mitigate these risks. Current clinical practices involve administration of systemic anticoagulants, the most common of which is unfractionated heparin [10, 11]. However, heparin is associated with risks including bleeding and a paradoxically prothrombotic state of heparin-induced thrombocytopenia [12, 13]. The risks of systemic anticoagulation motivate efforts to improve the hemocompatibility of oxygenators by applying antithrombotic coatings, including heparin analogs and albumin, to oxygenator surfaces [14–16].

To evaluate the prothrombotic effects of membrane oxygenator material and structural properties, we aimed to establish a rigorous method for quantifying thrombus formation in these devices. Previous studies have demonstrated the utility of multidetector computed tomography and microcomputed tomography (microCT) for visualizing thrombi within oxygenators [17, 18]. Herein we build on this approach to provide a quantitative approach to compute the volume and surface area of thrombus formation with fouled ECMO oxygenators. We demonstrate the feasibility of our approach with a pilot analysis of 18 membrane oxygenators collected from 17 patients on ECMO. This method holds potential to serve as a tool for the evaluating the hemocompatibility of new biomaterials or effectiveness of pharmacological approaches to prevent or reduce the incidence of vascular device-associated thrombosis.

#### **Methods**

### Patient Enrollment and Demographic Data Collection

This study was approved by the Oregon Health & Science University Institutional Review Board prior to initiation (STUDY00025349, approved 2/8/2023). The study included patients of ages 18 years and older, receiving veno-venous (VV) or veno-arterial (VA) ECMO for any indication. ECMO circuits included square or circular oxygenators. Square oxygenator models were HLS Set Advanced or



### ECMO Decannulation and Membrane Oxygenator Collection

The ECMO flow rate was adjusted to 1-2 L/min prior to decannulation. After weaning the patient from ECMO, the drainage and return tubing was clamped and cut. Normal saline solution (0.9% NaCl) was immediately added to the cut ends of the tubing to remove air, and the tube ends were connected with a 3/8"×3/8" straight CPB connector (LivaNova) to form a closed loop, separating the ECMO circuit from the patient. Both cut ends of the circuit were completely filled with saline before forming the loop, ensuring a 'wet-to-wet' connection to maintain a continuous liquid phase and prevent air ingress. Alternatively, before reopening or reconnecting the circuit, the connection was submerged in a saline-filled container to preserve the liquid interface. After patient separation, normal saline was pumped at 1-2 L/min for 5 minutes to flush excess blood.

#### **Membrane Oxygenator Processing**

Membrane oxygenators were removed from the collected ECMO circuits and fixed by dispensing 300 mL of 4% paraformaldehyde in 0.1 M phosphate-buffered saline (PBS) into the casing with a syringe. Oxygenators were stored in paraformaldehyde for 24–48 hours. We designed custom vise clamps to maintain the structure of the square oxygenators while cutting away the outer casing with a stainless-steel bandsaw (Lenox Classic Bi-Metal blade, 8/12 TPI). The square oxygenators measured 160 mm×160 mm×90 mm with casing and 90 mm×90 mm×55 mm after casing removal. The metal relief spring and other remaining components were removed from the oxygenator prior to microCT imaging to prevent image distortions.

For processing circular oxygenators, we cut and removed the plastic casing from both ends of the oxygenator, leaving the thin casing along the side of the cylinder. We removed the metal heating rod from the center of the membrane oxygenators then cut along the vertical axis, forming two halfcylinders, to accommodate the microCT system dimensions.

Oxygenators were removed from formaldehyde solution 24 hours prior to imaging and immersed in Lugol solution



(L6146, Sigma Aldrich). Lugol solution, which is comprised of aqueous potassium iodide and iodine, was used as a contrast agent to enhance the microCT imaging of the cellular components and structure of the thrombi within the oxygenator [19, 20].

#### Micro-computed Tomography

We imaged oxygenators using an Inveon MicroCT system (Siemens) with a 14-bit x-ray imaging detector with  $4,096 \times 4,096$  pixels, scanning at 4.65 degree intervals. We acquired stacks of 1,024 images for all three spatial dimensions with a voxel size of  $98.731 \, \mu m$  and standardized imaging parameters ( $80 \, kV$  voltage,  $114 \, \mu A$  intensity,  $1,200 \, ms$  integration time). The acquisition field of view covered a total area of  $100 \, mm \times 100 \, mm$ .

#### **Thrombus Quantification**

We performed image reconstruction and segmentation using Dragonfly software version 2022.2 (Comet Technologies Canada Inc.). We calibrated the contrast window to a range of 0-600 Hounsfield units (HU). To quantify thrombus deposition within each structurally distinct layer of the square oxygenators, we segmented thrombus areas in three randomly selected frontal view slices from each layer. The oxygenator was delineated with a lower threshold of 150 HU, and thrombi were delineated with a lower threshold between 310 HU and 415 HU. We manually adjusted this segmentation to annotate all deposits in each slice and calculated the average percent area of thrombus deposition across the selected slices in each layer.

To visualize the three-dimensional distribution of thrombus deposition and quantify thrombus volume, we performed density mapping of the entire square oxygenator and of each layer. We again delineated thrombus regions with a lower threshold between 310 HU and 415 HU and calculated the percent volume of thrombus deposition. Circular oxygenators have a uniform structure, lacking the distinct layers found in square oxygenators; therefore, we only performed three-dimensional quantification on these devices. We applied the same density mapping and thresholding steps as described for square oxygenators to delineate thrombi and calculate percent volume of thrombus deposition in circular oxygenators

#### Scanning Electron Microscopy of Thrombi

After microCT imaging, we collected thrombi from each layer including hollow fibers at layer 2 of the square oxygenators and from the uniform hollow fiber layer of the circular oxygenators for visualization with scanning electron microscopy (SEM) and histological staining. Thrombi

collected for SEM were immersed in 4% formaldehyde in 0.1 M PBS on a shaker at room temperature overnight. Thrombi were then washed in a series of cold ethanol mixtures (50%, 70%, 80%, 90%, 95%, and 100% ethanol in water), each for 5 minutes on an orbital shaker at low speed. Samples were critical point dried (CPD300, Leica Biosystems) with 35 carbon dioxide exchange cycles, sputtered with platinum coating, and mounted with carbon glue. We imaged thrombi on a Volumescope 2 SEM (Thermo Fisher Scientific) with a directional backscatter detector under  $800 \times$ ,  $1,000 \times$ , and  $2,000 \times$  magnifications (7.00 kV voltage, 6.5-6.9 mm work distance). Mountains® 10.3 (Digital Surf Inc.) was used for qualitative analysis of SEM images to assess pore, fibrin, and blood cell areas. The 'analyze pore, particles, and fibrin' command was applied, using a fixed signal threshold as a positive signal. Additionally, any area exceeding 1 µm<sup>2</sup> was also considered a positive signal.

#### **Histological Staining of Thrombi**

Thrombi collected for histological staining were prepared using a standard tissue processing protocol, embedded in paraffin, and cut into 4  $\mu$ m sections. Representative sections were stained with hematoxylin and eosin (H&E) to examine thrombus composition. Whole slide scanning was performed on an Aperio AT Turbo digital pathology scanner (Leica Biosystems), to identify thrombus composition such as red blood cell and fibrin content qualitatively.

#### **Results**

#### **Patient Enrollment and Oxygenator Collection**

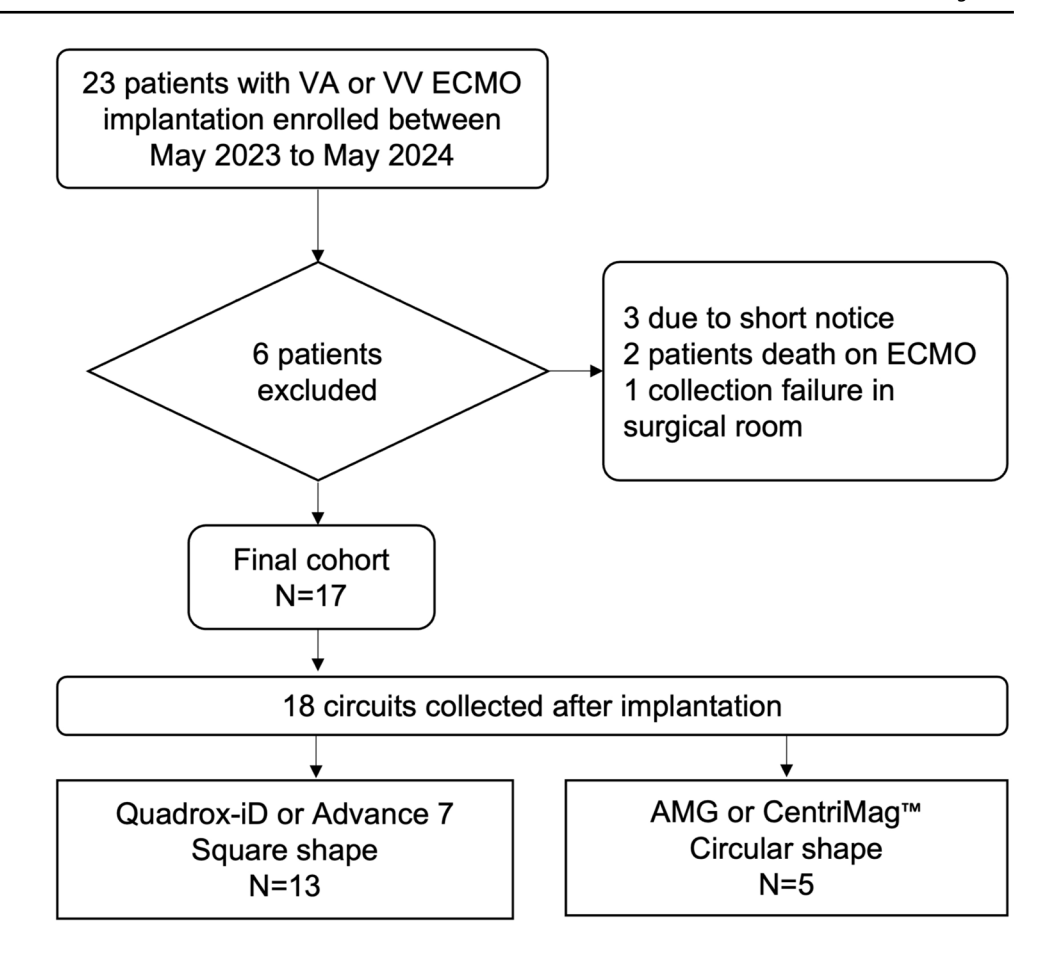
From an initial cohort of 23 patients, we excluded 6 patients due to short notice prior to decannulation, patient death during ECMO support, or failure in collecting oxygenators (Figure 1). Our final dataset included 17 patients. Patient demographics are listed in Supplemental Table 1. We collected two oxygenators from one of these patients, yielding a total of 18 oxygenators available for analysis, including 13 square oxygenators and 5 circular oxygenators. All patients received systemic anticoagulation with heparin or a combination of heparin and bivalirudin.

Oxygenators were disconnected from patients and rinsed with saline at the bedside. One of the six patients excluded was due to a failure during oxygenator collection, in which air accidentally entered the ECMO circuit after decannulation. Thus, we chose to exclude this oxygenator from our analysis.



200 J. S. H. Wang et al.

**Fig. 1** Patient enrollment for ECMO circuit collection study



#### Histological Staining and Scanning Electron Microscopy

We identified five structurally distinct layers within the square oxygenators. We performed SEM and histological staining on thrombi extracted from the first two layers in the direction of blood flow. H&E staining indicates accumulation of erythrocytes in thrombi in the first layer of the oxygenator (Fig. 2a). Thrombi originally collected from the first layer of the square oxygenator are shown in Fig. 2g. Thrombi from the second layer were primarily composed of fibrin and contained fewer erythrocytes (Fig. 2b, h). SEM images supported these findings and revealed structural details including the presence of polyhedral erythrocytes, fibrin, and pores, characteristic features of thrombi (Fig. 2c and d) [21]. We quantified the SEM images by labeling the areas of blood cells, fibrin, and pores (Figure 2h). The first layer demonstrates a higher proportion of blood cells (25.4%) and lower fibrin content (22.6%), whereas the second layer, where the fine-structure hollow fiber is located, is characterized by a substantial increase in fibrin deposition (49.0%) and a marked reduction in blood cell presence (0.9%). This pattern suggests that thrombus formation within the oxygenator exhibits a configuration-relevant gradient. Here we also highlighted significant thrombus formation on the ties linking the hollow fibers within the second layer (Fig. 2e and f).

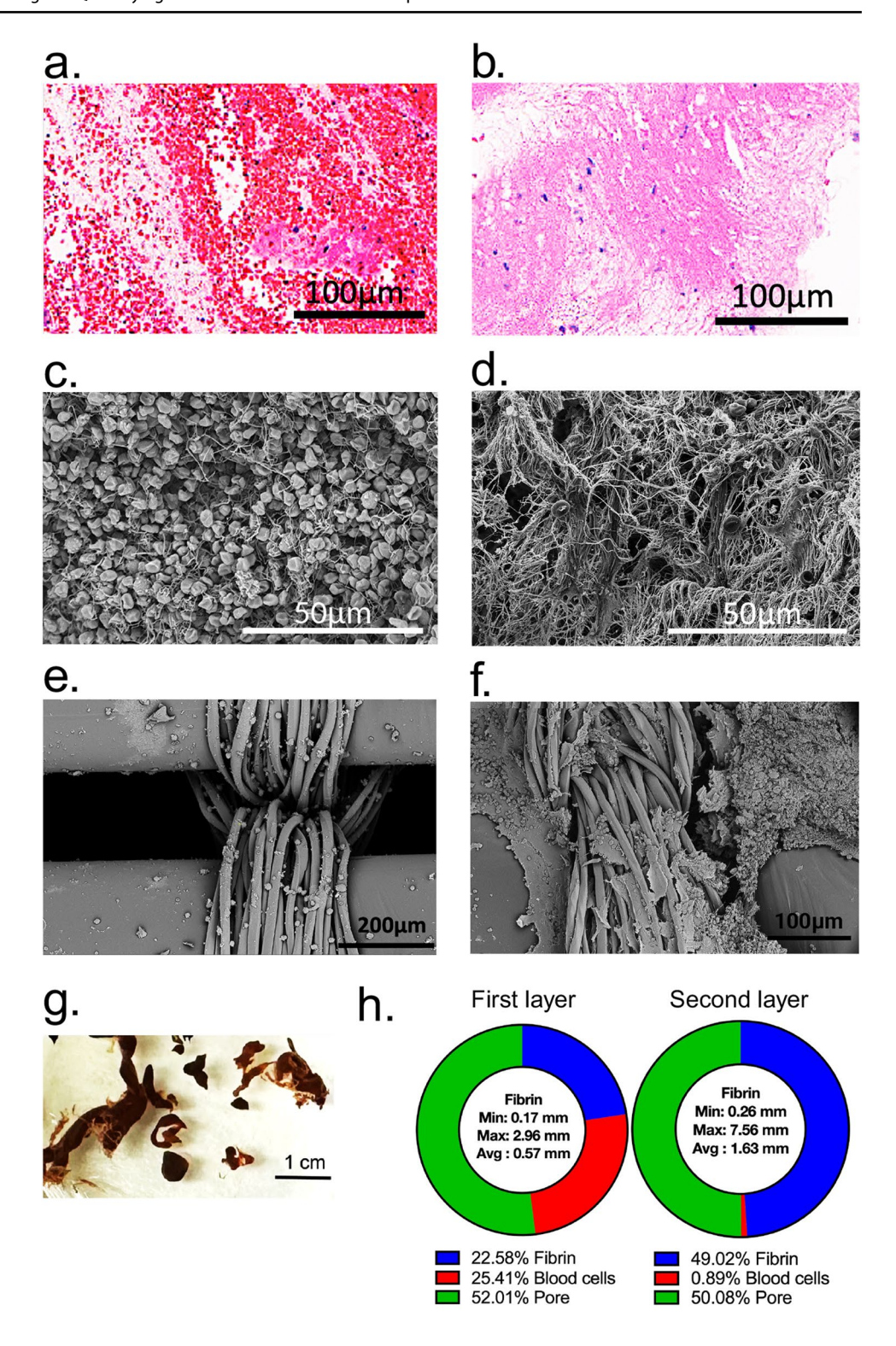
Unlike the layered square oxygenators, circular oxygenators have a uniform structure. SEM and histological staining were performed on thrombi extracted from the membrane in the direction of blood flow. A large thrombus was found where blood flows into the area of the ECMO, and centrifugal force caused its distribution toward the outer side, as shown in Fig. 2i. H&E staining indicates the accumulation of erythrocytes and fibrin tightly mixed in thrombi in the blood inflow region of the oxygenator (Fig. 2j). As in the square oxygenators, SEM images showed polyhedral erythrocytes, platelets, fibrin, and pores (Fig. 2k and l). The porosity is lower in the thrombus of circular oxygenators than in square oxygenators. (Fig. 2n). Again, blood cells and thrombus accumulated on the ties linking the hollow fibers (Fig. 2m).

### Two-dimensional Quantification in Square Oxygenators

To investigate the spatial distribution of thrombus formation within an oxygenator, we developed a method for visualizing and quantifying thrombus area through microCT imaging (Fig. 3). After collection from patients



Fig. 2 Histological staining and SEM images show thrombus formation in ECMO oxygenator layers. In the first layer (a), erythrocyte-rich thrombi are observed, while the second layer (b) shows fibrin-dominant thrombi. H&E staining highlights thrombus composition in the ECMO layers. SEM images (c-f) show polyhedral erythrocytes in the first layer (c) and thrombus buildup on fiber ties in the second layer at  $1000 \times (e)$ and  $2000 \times (\mathbf{f})$  magnifications. g shows human clots from the first layer of square ECMO, and h shows SEM analysis of clot composition in the first and second layers. i and j show thrombus photo and H&E staining from the blood inflow region of circular ECMO. SEM analysis k-l reveals twisted thrombus structures, including erythrocytes and fibrin, at 800×and 2000×magnification. m thrombus attached amount on fiber ties n shows SEM analysis of clot composition and pore percentages in circular ECMO

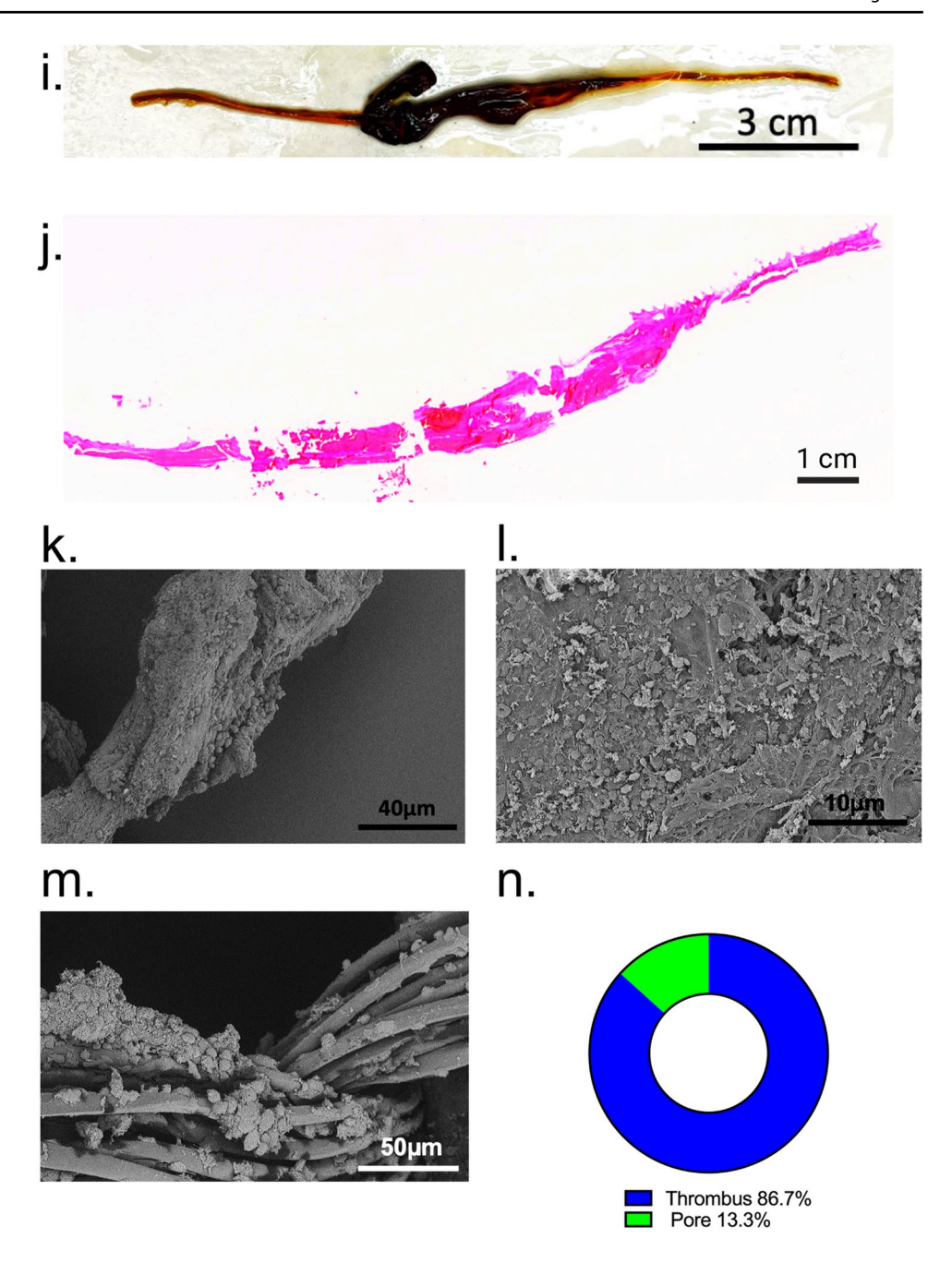


requiring ECMO, oxygenators were fixed with paraformaldehyde and removed from the exterior casing for microCT imaging. We reconstructed microCT images and identified five distinct layers with different structural patterns in the square oxygenators (Fig. 4a). We analyzed samples of three frontal view slices within each layer to calculate the average percent area of thrombus deposition by layer. Our results indicate that Layer 2 of these oxygenators, the second layer in the direction of blood flow, contained the highest average percent area of thrombotic formation (Fig. 4c).



J. S. H. Wang et al.

Fig. 2 (continued)



## Three-Dimensional Quantification in Square and Circular Oxygenators

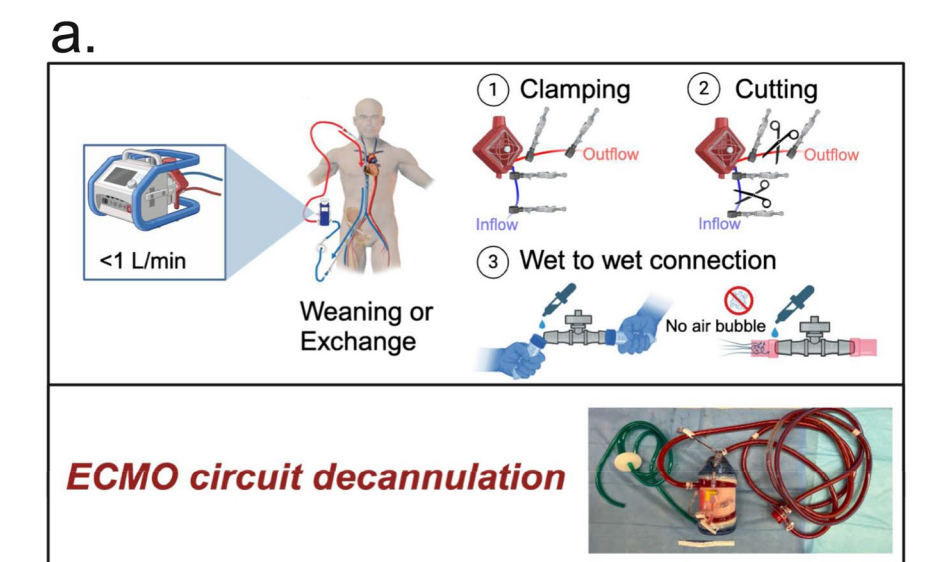
We extended our segmentation method to three-dimensional reconstructions to quantify thrombus volumes from density mapping of oxygenators. We again isolated five layers and calculated the percent thrombus volume within each layer (Fig. 5a). We also calculated the total percent thrombus volume throughout each whole oxygenator. This total thrombus volume offers a metric for assessing overall thrombus deposition in oxygenators across various device parameters and clinical factors. As an example, we present

thrombus volumes with the duration of use for each oxygenator (Fig. 5b). We imaged an unused oxygenator that had not been exposed to blood for establishing a baseline by applying the same segmentation process used for the fouled oxygenators (Supplemental Figure 1).

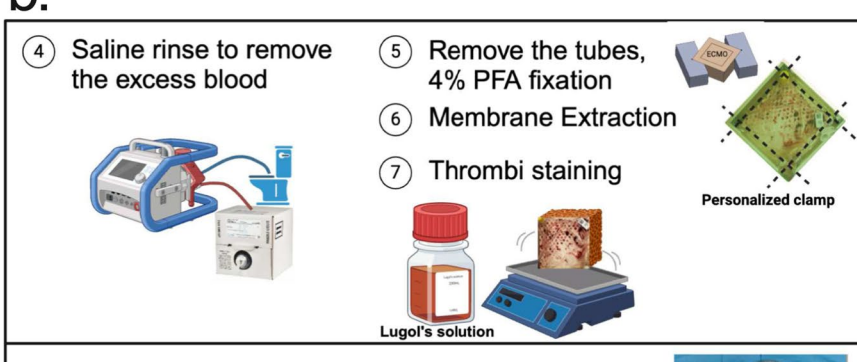
We next applied the three-dimensional quantification method to circular oxygenators, which are homogenous unlike the layered square oxygenators. We reconstructed microCT images of circular oxygenators, combining images from both half-cylinders for each oxygenator. We performed density mapping of thrombus spatial distribution and segmentation of thrombotic deposits and quantified the overall



Fig. 3 Collection and imaging methods for ECMO circuit thrombi. a ECMO circuit decannulation using clamping, cutting, and wet-to-wet connection. b Thrombi fixation and staining with saline rinse, PFA fixation, and Lugol's solution. c CT scan and 3D image segmentation of thrombi, with axial, sagittal, and frontal views



b.



### Thrombi fixation and staining



C.

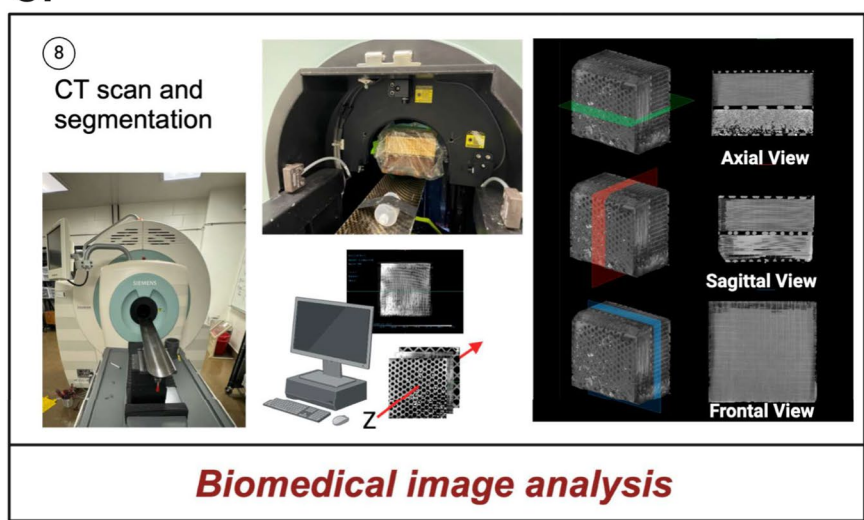
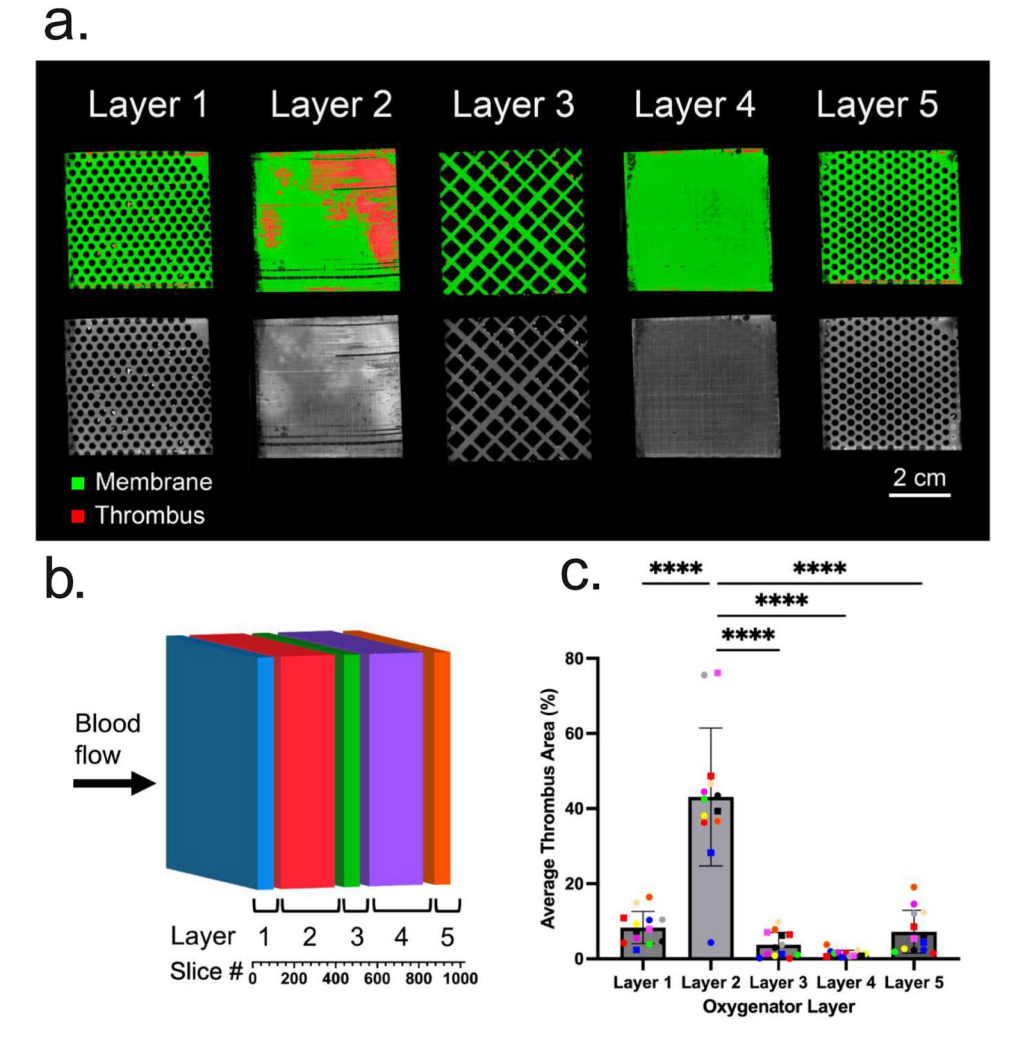




Fig. 4 2D quantification of thrombus in oxygenator layers. a Thrombus (red) and membrane (green) distribution across the five oxygenator layers. b 3D illustration showing thrombus distribution in the ECMO region, correlated with CT scan slices along the direction of blood flow. c Quantification of thrombus area, with most thrombi found in layers 1 and 2 (\*\*\*\*p<0.0001)



percent volume of deposits throughout each circular oxygenator (Fig. 6a). These results indicate accumulation of high density thrombus near where the blood enters the cylinder and variation in thrombus volume across durations of oxygenator use (Fig. 6b). Like the unused square oxygenator, we found no thrombi when applying the same segmentation process used for the fouled oxygenators (Supplemental Figure 2). Overall, we quantified thrombus formation by analyzing the thrombus spatial distribution in whole ECMO components and calculating thrombus volume percentage for multiple shapes of used ECMO oxygenators.

#### **Discussion**

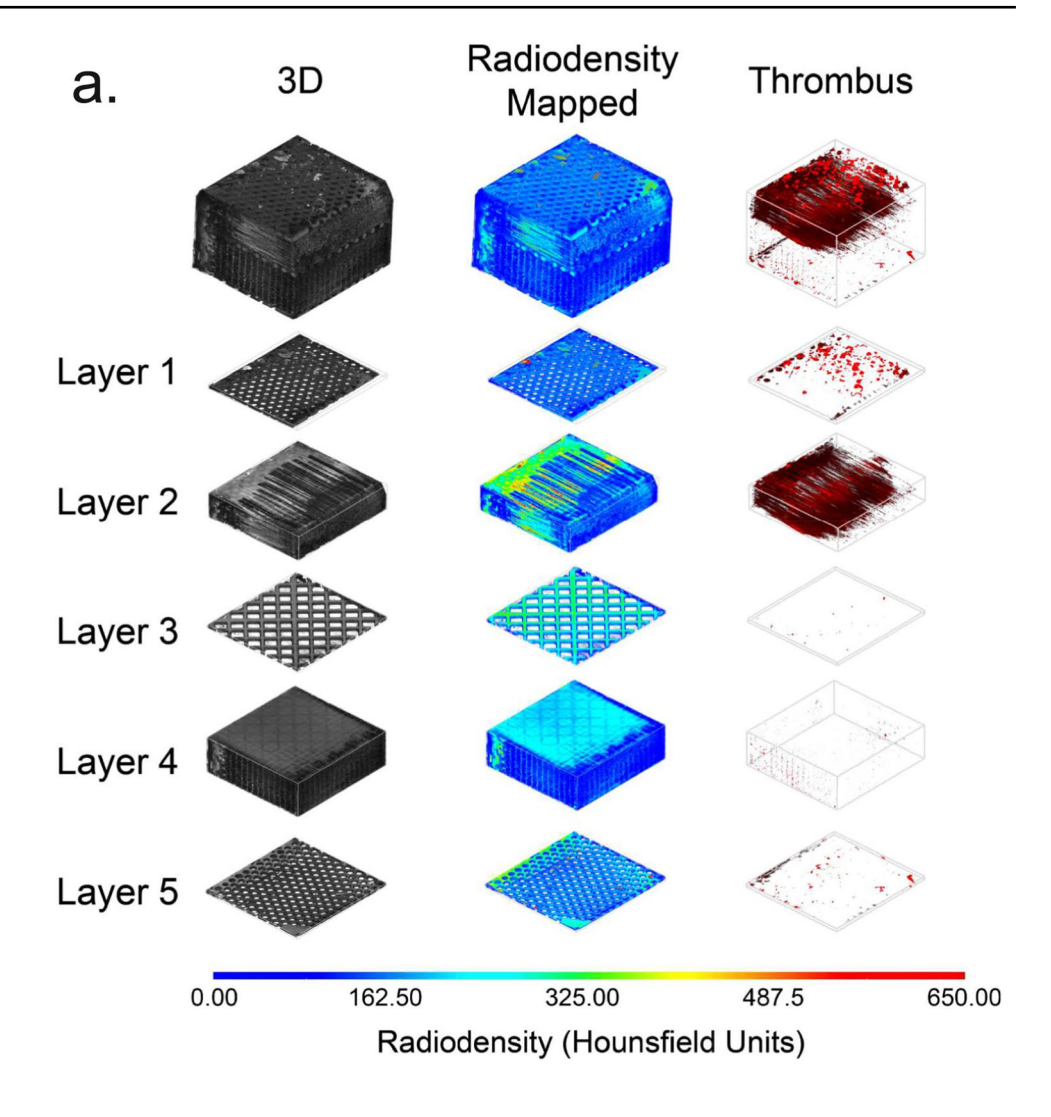
Collection, imaging, and quantitative analysis of used ECMO oxygenators will enable the investigation of the structural properties of membrane oxygenators and the three-dimensional distribution of thrombus formation with these medical devices. Our results indicate thrombus accumulation within the initial days of ECMO treatment, with

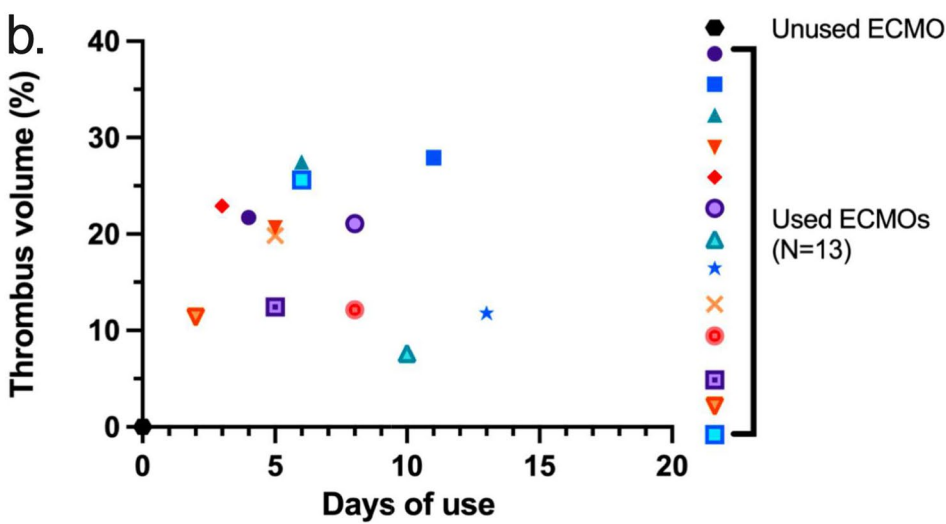
the extent of accumulation varying between regions of the oxygenator. This new method of oxygenator collection and analysis complements standard microscopy techniques to yield insights on structural and material features that may contribute to oxygenator thrombosis.

ECMO treatment involves a high risk of thrombotic complications [22, 23]. Contact between blood and materials within the circuit promotes activation and consumption of coagulation factors, leading to thrombosis and hemorrhage [6]. Thrombus deposition within the membrane oxygenator can increase mechanical resistance in diffusion capillaries and reduce the gas exchange capacity of the oxygenator, further complicating extended ECMO use. Moreover, medical device-induced thrombosis can exacerbate systemic inflammation through activation of the contact system of coagulation, neutrophils, and platelets [13, 24]. Proinflammatory cytokines are associated with an increased risk of mortality during ECMO treatment [25, 26]. Improvements to ECMO membrane designs or novel anticoagulants to prevent contact pathway activation may address the critical risks of medical device-induced thrombosis [27–29].



Fig. 5 3D quantification of thrombus in square oxygenator. a 3D visualization of radiodensity mapping and thrombus distribution across oxygenator layers 1–5, with higher thrombus accumulation in the first two layers. b Thrombus volume over days of ECMO use, showing increased thrombus formation with prolonged usage compared to unused ECMO circuits (N=13)





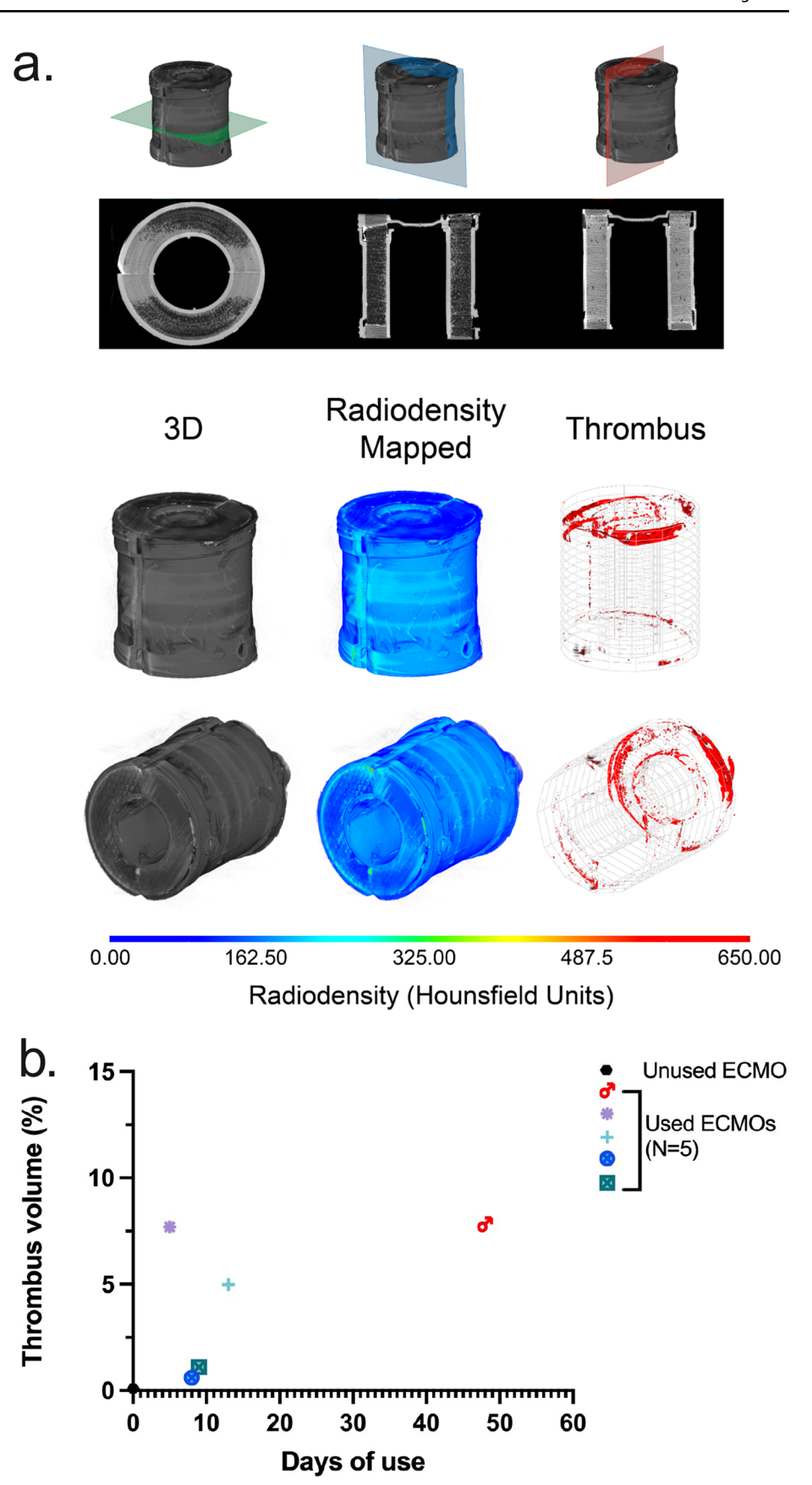
The emergency use of ECMO as therapy creates a challenge for membrane collection in a critical care setting. It is complicated to predict when a patient will require

decannulation, and therefore difficult to prepare laboratory materials before collection. This also holds true for blood collection to monitor the temporal pattern of activation of



J. S. H. Wang et al.

Fig. 6 3D quantification of thrombus in circular oxygenator. a 3D reconstruction, radiodensity mapping, and thrombus distribution in a circular oxygenator. b Thrombus volume (%) increases with ECMO usage duration (N=5)





coagulation factors and blood cells. Moreover, complications during the weaning process may require that the patient be reconnected to ECMO support, preventing oxygenator collection. After decannulation, there is a risk of clotting throughout the disconnected ECMO circuit. We prevented clotting during collection by using a bulb syringe to fill the cut ends of the circuit with saline and connecting the two ends to continue circulation through the ECMO system. We found it necessary to quickly form this closed circuit to prevent introduction of air into the ECMO tubing to prevent artefactual clotting. One limitation of our collection method is that this saline rinse may remove or disrupt some thrombotic deposits from the membrane, resulting in an underestimation of the thrombus volume present during ECMO treatment. A key limitation of this study is the lack of systematically collected patient oxygenation data, such as arterial blood gas measurements and continuous pulse oximetry, which prevented an analysis of the potential correlation between thrombus volume and patient oxygenation status. An additional limitation is the variability in anticoagulant management arising from patient-specific adjustments and clinical monitoring. Although anticoagulant infusion rates and anti-factor Xa concentrations were monitored following established guidelines, the absence of real-time data limits the accuracy of this aspect.

In conclusion, we developed a method of oxygenator collection and thrombus quantification for the assessment of the extent and distribution of thrombosis during ECMO. Future applications of this method can include analyses of the relationships between blood flow patterns, treatment methods, and the cellular makeup of thrombus accumulation [30]. Quantification of thrombotic deposits may enable improved monitoring of patient outcomes to understand the progression of thrombotic complications and evaluate clinical strategies. Analysis of the spatial distribution of deposits can provide details on structural and material factors driving oxygenator thrombosis. These insights may facilitate development and evaluation of ECMO technologies to reduce risks for patients receiving critical care.

**Supplementary Information** The online version contains supplementary material available at https://doi.org/10.1007/s12195-025-00847-0.

**Acknowledgements** This work is supported in part by the National Institute of Health Heart, Lung, and Blood Institute (R01HL144133, R01HL101972, R01HL151367, and R01HL168696) and the Institute of Allergy and Infectious Diseases (R01AI157037).

Author Contributions Conceived and designed experiments: J.S.H.W., R.R., S.R., A.L.K., J.J.S., O.J.T.M. Performed experiments: J.S.H.W., H.H.V., B.Z., D.Z., R.R. Analyzed the data: J.S.H.W., C.H.M., A.L., A.L.K. Wrote and edited the manuscript: J.S.H.W., A.A.R., S.R., B.Z., D.Z., R.R., A.K., D.W., O.J.T.M., A.L.K., J.J.S.

Data Availability The data supporting the findings of this study are available upon request.

#### **Declarations**

Conflict of interest All other authors declare no potential conflicts of interest.

Research Invovling Human and Animal Participant All procedures followed were in accordance with the ethical standards of the responsible committee on human experimentation (institutional and national) and with the Helsinki Declaration. No laboratory animals were used in this study.

**Informed Consent** Informed consent was obtained from all patients for being included in the study. This study was approved by the Oregon Health & Science University Institutional Review Board prior to initiation (STUDY00025349).

#### References

- Bartlett, R., D. J. Arachichilage, M. Chitlur, S. R. Hui, C. Neunert, A. Doyle, et al. The History of Extracorporeal Membrane Oxygenation and the Development of Extracorporeal Membrane Oxygenation Anticoagulation. *Semin Thromb Hemost.* 50:81–90, 2024. https://doi.org/10.1055/s-0043-1761488.
- Punjabi, P. P., and K. M. Taylor. The science and practice of cardiopulmonary bypass: From cross circulation to ECMO and SIRS. *Glob Cardiol Sci Pract*. 2013:249–260, 2013. https://doi.org/10. 5339/gcsp.2013.32.
- Xu, Z., Y. Xu, D. Liu, X. Liu, L. Zhou, Y. Huang, et al. Case Report: Prolonged VV-ECMO (111 Days) Support in a Patient With Severe COVID-19. Front Med (Lausanne). 8:681548, 2021. https://doi.org/10.3389/fmed.2021.681548.
- Broman LM, Dubrovskaja O, Balik M. Extracorporeal Membrane Oxygenation for Septic Shock in Adults and Children: A Narrative Review. J Clin Med. 2023;12. https://doi.org/10.3390/jcm12 206661
- Austin, S. E., S. M. Galvagno, J. E. Podell, W. A. Teeter, R. Kundi, D. J. Haase, et al. Venovenous extracorporeal membrane oxygenation in patients with traumatic brain injuries and severe respiratory failure: A single-center retrospective analysis. *J Trauma Acute Care Surg.* 96:332–339, 2024. https://doi.org/10.1097/TA.00000 00000004159.
- Goel, A., H. Tathireddy, S. H. Wang, H. H. Vu, C. Puy, M. T. Hinds, et al. Targeting the Contact Pathway of Coagulation for the Prevention and Management of Medical Device-Associated Thrombosis. Semin Thromb Hemost. 2023. https://doi.org/10. 1055/s-0043-57011.
- Doyle, A. J., and B. J. Hunt. Current Understanding of How Extracorporeal Membrane Oxygenators Activate Haemostasis and Other Blood Components. Front Med (Lausanne). 5:352, 2018. https://doi.org/10.3389/fmed.2018.00352.
- Kim, T. W., R. E. Ko, K. H. Choi, C. R. Chung, Y. H. Cho, and J. H. Yang. Overt disseminated intravascular coagulation and antithrombin III predict bleeding and in-hospital mortality in patients undergoing extracorporeal membrane oxygenation. *Front Med* (*Lausanne*). 11:1335826, 2024. https://doi.org/10.3389/ fmed.2024.1335826.
- Papageorgiou, C., G. Jourdi, E. Adjambri, A. Walborn, P. Patel, J. Fareed, et al. Disseminated Intravascular Coagulation: An Update on Pathogenesis, Diagnosis, and Therapeutic Strategies. *Clin Appl Thromb Hemost.* 24:8s–28s, 2018. https://doi.org/10.1177/10760 29618806424.
- McMichael, A. B. V., L. M. Ryerson, D. Ratano, E. Fan, D. Faraoni, and G. M. Annich. 2021 ELSO Adult and Pediatric



- Anticoagulation Guidelines. *Asaio j.* 68:303–310, 2022. https://doi.org/10.1097/MAT.0000000000001652.
- Akbulut, A. C., R. A. Arisz, C. Baaten, G. Baidildinova, A. Barakzie, R. Bauersachs, et al. Blood Coagulation and Beyond: Position Paper from the Fourth Maastricht Consensus Conference on Thrombosis. *Thromb Haemost.* 123:808–839, 2023. https://doi.org/10.1055/a-2052-9175.
- Giuliano, K., B. F. Bigelow, E. W. Etchill, A. K. Velez, C. S. Ong, C. W. Choi, et al. Extracorporeal Membrane Oxygenation Complications in Heparin- and Bivalirudin-Treated Patients. *Crit Care Explor.* 3:e0485, 2021. https://doi.org/10.1097/CCE.00000 00000000485.
- Kohs, T. C. L., P. Liu, V. Raghunathan, R. Amirsoltani, M. Oakes, O. J. T. McCarty, et al. Severe thrombocytopenia in adults undergoing extracorporeal membrane oxygenation is predictive of thrombosis. *Platelets*. 33:570–576, 2022. https://doi.org/10.1080/ 09537104.2021.1961707.
- Coronel-Meneses, D., C. Sánchez-Trasviña, I. Ratera, and K. Mayolo-Deloisa. Strategies for surface coatings of implantable cardiac medical devices. *Front Bioeng Biotechnol.* 11:1173260, 2023. https://doi.org/10.3389/fbioe.2023.1173260.
- Kartika, T., R. Mathews, G. Migneco, T. Bundy, A. J. Kaempf, M. Pfeffer, et al. Comparison of bleeding and thrombotic outcomes in veno-venous extracorporeal membrane oxygenation: Heparin versus bivalirudin. *Eur J Haematol*. 112:566–576, 2024. https:// doi.org/10.1111/ejh.14146.
- Kohs, T. C. L., B. R. Weeder, B. I. Chobrutskiy, T. Kartika, K. K. Moore, O. J. T. McCarty, et al. Predictors of thrombosis during VV ECMO: an analysis of 9809 patients from the ELSO registry. *J Thromb Thrombolysis*. 57:345–351, 2024. https://doi.org/10.1007/s11239-023-02909-4.
- Dornia, C., A. Philipp, S. Bauer, P. Hoffstetter, K. Lehle, C. Schmid, et al. Visualization of thrombotic deposits in extracorporeal membrane oxygenation devices using multidetector computed tomography: a feasibility study. *Asaio j.* 59:439–441, 2013. https://doi.org/10.1097/MAT.0b013e3182976eff.
- Birkenmaier, C., C. Dornia, K. Lehle, T. Müller, M. Gruber, A. Philipp, et al. Analysis of Thrombotic Deposits in Extracorporeal Membrane Oxygenators by High-resolution Microcomputed Tomography: A Feasibility Study. *Asaio j.* 66:922–928, 2020. https://doi.org/10.1097/MAT.000000000001089.
- Degenhardt, K., A. C. Wright, D. Horng, A. Padmanabhan, and J. A. Epstein. Rapid 3D phenotyping of cardiovascular development in mouse embryos by micro-CT with iodine staining. *Circ Cardiovasc Imaging*. 3:314–322, 2010. https://doi.org/10.1161/ CIRCIMAGING.109.918482.
- Gignac, P. M., N. J. Kley, J. A. Clarke, M. W. Colbert, A. C. Morhardt, D. Cerio, et al. Diffusible iodine-based contrast-enhanced computed tomography (diceCT): an emerging tool for rapid, high-resolution, 3-D imaging of metazoan soft tissues. *J Anat.* 228:889–909, 2016. https://doi.org/10.1111/joa.12449.
- Tutwiler, V., A. R. Mukhitov, A. D. Peshkova, G. Le Minh, R. R. Khismatullin, J. Vicksman, et al. Shape changes of erythrocytes during blood clot contraction and the structure of

- polyhedrocytes. *Sci Rep.* 8:17907, 2018. https://doi.org/10.1038/s41598-018-35849-8.
- Olson, S. R., C. R. Murphree, D. Zonies, A. D. Meyer, O. J. T. McCarty, T. G. Deloughery, et al. Thrombosis and Bleeding in Extracorporeal Membrane Oxygenation (ECMO) Without Anticoagulation: A Systematic Review. *Asaio j.* 67:290–296, 2021. https://doi.org/10.1097/MAT.000000000001230.
- Chlebowski, M. M., S. Baltagi, M. Carlson, J. H. Levy, and P. C. Spinella. Clinical controversies in anticoagulation monitoring and antithrombin supplementation for ECMO. *Critical Care*. 24:19, 2020. https://doi.org/10.1186/s13054-020-2726-9.
- Kharnaf, M., F. Zafar, S. Hogue, L. Rosenfeldt, R. L. Cantrell, B. K. Sharma, et al. Factor XII promotes the thromboinflammatory response in a rat model of venoarterial extracorporeal membrane oxygenation. *J Thorac Cardiovasc Surg.* 168:e37–e53, 2024. https://doi.org/10.1016/j.jtcvs.2023.08.045.
- Al-Fares, A., T. Pettenuzzo, and L. Del Sorbo. Extracorporeal life support and systemic inflammation. *Intensive Care Med Exp.* 7:46, 2019. https://doi.org/10.1186/s40635-019-0249-y.
- Hatami, S., J. Hefler, and D. H. Freed. Inflammation and Oxidative Stress in the Context of Extracorporeal Cardiac and Pulmonary Support. Front Immunol. 13:831930, 2022. https://doi.org/10. 3389/fimmu.2022.831930.
- Meyer, A. D., C. R. Thorpe, T. Fraker, T. Cancio, J. Rocha, R. P. Willis, et al. Factor XI Inhibition With Heparin Reduces Clot Formation in Simulated Pediatric Extracorporeal Membrane Oxygenation. *Asaio j.* 69:1074–1082, 2023. https://doi.org/10.1097/MAT.0000000000002048.
- Wallisch, M., C. U. Lorentz, H. H. S. Lakshmanan, J. Johnson, M. R. Carris, C. Puy, et al. Antibody inhibition of contact factor XII reduces platelet deposition in a model of extracorporeal membrane oxygenator perfusion in nonhuman primates. *Res Pract Thromb Haemost*. 4:205–216, 2020. https://doi.org/10.1002/rth2. 12309
- Raghunathan, V., P. Liu, T. C. L. Kohs, R. Amirsoltani, M. Oakes, O. J. T. McCarty, et al. Heparin Resistance Is Common in Patients Undergoing Extracorporeal Membrane Oxygenation but Is Not Associated with Worse Clinical Outcomes. *Asaio j.* 67:899–906, 2021. https://doi.org/10.1097/MAT.000000000001334.
- Kim, D. A., and D. N. Ku. Structure of shear-induced platelet aggregated clot formed in an in vitro arterial thrombosis model. *Blood Adv.* 6:2872–2883, 2022. https://doi.org/10.1182/blood advances.2021006248.

**Publisher's Note** Springer Nature remains neutral with regard to jurisdictional claims in published maps and institutional affiliations.

#### **Authors and Affiliations**

Jenny S. H. Wang $^1 \odot \cdot$  Amelia A. Rodolf $^1 \cdot$  Caleb H. Moon $^1 \cdot$  Ari Lauthner $^1 \cdot$  Helen H. Vu $^1 \cdot$  Sandra Rugonyi $^1 \cdot$  Anna J. Hansen $^2 \cdot$  Heather M. Mayes $^3 \cdot$  Bishoy Zakhary $^4 \cdot$  David Zonies $^5 \cdot$  Ran Ran $^{4,6} \cdot$  Akram Khan $^4 \cdot$  Denis Wirtz $^{7,8,9,10,11} \cdot$  Ashley L. Kiemen $^{7,8,11,12,13} \cdot$  Owen J. T. McCarty $^1 \cdot$  Joseph J. Shatzel $^{1,14}$ 

☑ Jenny S. H. Wang wangsi@ohsu.edu

Department of Biomedical Engineering, Oregon Health & Science University, 3303 S Bond Ave, Portland, OR 97239, USA



- Division of Nursing, Cardiovascular Intensive Care, Oregon Health & Science University, Portland, OR, USA
- Division of Nursing, Oregon Health & Science University, Portland, OR, USA
- Division of Pulmonary and Critical Care Medicine, Oregon Health & Science University, Portland, OR, USA
- Department of Surgery, University of Washington, Seattle, WA, USA
- Department of Emergency Medicine, Oregon Health & Science University, Portland, OR, USA
- Department of Chemical and Biomolecular Engineering, Johns Hopkins University, Baltimore, MD, USA
- Johns Hopkins Institute for NanoBioTechnology, Johns Hopkins University, Baltimore, MD, USA

- Johns Hopkins Physical Sciences-Oncology Center, Johns Hopkins University, Baltimore, MD, USA
- Department of Oncology, Johns Hopkins School of Medicine, Baltimore, MD, USA
- Department of Pathology, Sol Goldman Pancreatic Cancer Research Center, Johns Hopkins School of Medicine, Baltimore, MD, USA
- Sidney Kimmel Comprehensive Cancer Center, Johns Hopkins School of Medicine, Baltimore, MD, USA
- Department of Functional Anatomy & Evolution, Johns Hopkins School of Medicine, Baltimore, MD, USA
- Division of Hematology and Medical Oncology, Oregon Health & Science University, Portland, OR, USA

